Journal of Network Intelligence
Taiwan Ubiquitous Information
 ISSN 2414-8105 (Online)
Volume **8**, Number **1**, February **2023**

An Information Feedback-based Particle Swarm Optimization Algorithm for Multi-regional Image Segmentation

Fan-Qi Meng

School of computer science
Northeast Electric Power University
No.169 Changchun Road, Jilin City, Jilin Province, 132012, China
School of information engineering
Guangdong Atv Academy For Performing Arts
Huijing Road, Dongguan City, Guangdong Province, 523710, China
meng8191@163.com

Shuang Wei

School of computer science
Northeast Electric Power University
No.169 Changchun Road, Jilin City, Jilin Province, 132012, China
1411211016@qq.com

Jing-Dong Wang*

School of computer science
Northeast Electric Power University
No.169 Changchun Road, Jilin City, Jilin Province, 132012, China
20102248@neepu.edu.cn

Pei-Fang Wang

School of computer science
Northeast Electric Power University
No.169 Changchun Road, Jilin City, Jilin Province, 132012, China
w13578519072@163.com

Bin Li

School of computer science
Northeast Electric Power University
No.169 Changchun Road, Jilin City, Jilin Province, 132012, China
362383414@qq.com

*Corresponding author: Jing-Dong Wang
Received April 2, 2022, revised May 11, 2022, accepted August 3, 2022.

Abstract. *Multi-objective evolutionary algorithm (MOEA) is the most common algorithm in multi-regional image segmentation. More objectives should consider the image qualities more comprehensively. However, the optimization performance declines with the number of objective increases. Aiming at this problem, we establish a seven-objective model considering the quality of the image and proposed an information feedback-based particle swarm optimization (SMPSO-IFM) algorithm to solve the seven-objective model. The novelty lies in that the information feedback makes the SMPSO-IFM has the ability to alleviate the conflict between the objective functions so as to have better performance. We experiment with 100 images on the Berkeley Segmentation Dataset (BSDS300) and its performance is compared with the other four kinds of many-objective optimation (MaOP) algorithms applied in multi-regional image segmentation. We calculate the three performance indices of image segmentation. To verify the preponderance of SMPSO-IFM in MaOP, the algorithm was evaluated using a series of MAF and DTLZ benchmark problems. Extensive experimental results show that the proposed method is better to other algorithms so that the effectiveness and reasonability of SMPSO-IFM are verified.*
Keywords: Many-objective optimization, image segmentation, threshold segmentation, swarm optimization algorithm, information feedback model

1. **Introduction.** Many national and international researchers are dealing with image segmentation. It is one of the most difficult computer vision problems. The common methods of image segmentation include threshold-based image segmentation method [1], region-based image segmentation method [2], edge-based image segmentation method [3], active contour-based image segmentation [4], machine learning-based image segmentation [5] and so on. Among these methods, threshold segmentation is the most effective in terms of algorithmic complexity and image segmentation efficiency. The grayscale of something like an image is primarily used in the threshold segmentation method to identify an appropriate threshold value for segmentation into multiple regions. Because there are different gray levels, the image is split into two types with different grayscale area combinations. The equivalent binary picture can be generated by selecting an appropriate threshold value to identify whether each pixel in the image belongs to the target region or the background region, this method is called two-level threshold segmentation. However, if the image contains several objects with almost the same grayscale, it may not be sufficient to divide the image into two categories [6]. Therefore, more thresholds are required, so two-level thresholds should be extended to multi-level thresholds. This paper uses three thresholds to segment the image.

Several approaches for identifying the appropriate threshold value for a particular image have been offered. The Otsu method is widely recognized as the greatest algorithm for threshold selection in image segmentation [7], it calculates the variance to determine the appropriate grayscale value for the distribution using the clustering concept. Another popular algorithm is Kapur's method [8]. Kapur's method maximizes the variance and entropy between inter-classes in order to check the homogeneity of classes. However, many of these methods require more computation time when multiple thresholds are available. To address these issues, we tend to combine these methods with MOEAs. For instance, the ant colony algorithm [9], the particle swarm optimization [10], and the artificial bee colony algorithm [11]. Because the algorithm's performance degrades as the quantity of objective functions increases, a limited handful of objective functions is usually chosen to ensure the method's efficiency. The primary cause is that as the number of objectives increases, so does the number of non-dominant programs, leading to a lack of pressure on the Pareto frontier [12]. A multi-objective optimization algorithm (MOP) is presented as a consequence of this [13]. An optimization problem with two or three objectives is

usually called MOP, while a problem with four or more objectives is called MaOP. On the basis of the basic concept of MOP, many multi-objective threshold segmentation methods are proposed. For example, Multi-objective Multi-verse Optimization (MOMVO) was proposed as an image segmentation method that uses the Otsu function and Kapur's entropy function as objective functions [14]. Another is a very famous non-dominant genetic algorithm(NSGA-II) [15]. But the convergence and diversity of the algorithm are not good when facing the MOP of three or more objectives, the NSGA-II algorithm is improved and the NSGA-III algorithm is formed [16]. Multi-objective Evolutionary Algorithm Based on Decomposition (MOEA/D) has also been applied to this field [17]. PSO performs well in MaOPs because of its fast convergence speed and high efficiency, but it is effortless to run into locally optimal solutions. Speed-constrained particle swarm optimization(SMPSO) can avoid this problem [18]. During the iterations of the algorithm, only the greatest individuals in the final iteration are chosen and the rest are eliminated, this may lead to discarding useful information from the evolution of the population. The information feedback model can take advantage of the favorable information of the previous generation of particles to generate the new generation of particles to enhance the algorithm's performance. The paper's innovations are as follows: firstly, taking the image quality into account, we proposed a model considering seven objective functions, and then optimized the model using SMPSO combined with the information feedback model to eliminate the conflict between each objective and improve the algorithm performance.

The following are the paper's primary contributions:

(1) We treat the image segmentation problem as a MaOP problem. The objective function selects seven commonly used image segmentation functions.

(2) To determine the optimum way to eliminate conflicts between objectives, the SMPSO-IFM algorithm is utilized.

(3) To demonstrate the usefulness of our suggested algorithm, we compared its performance to other well-known MaOP algorithms.

The following is a list of the other chapters throughout this paper: Section 2 discusses related works on this topic. In Section 3, SMPSO-IFM is proposed. In Section 4, the experimental findings are analysed and compared to other MaOP methods. Section 5 summarizes the entire content and outlines the future work.

2. **Related works.**

2.1. **Problem definition.**

Many optimization issues in real life include numerous objectives, and these objectives frequently collide. An improvement in the performance of one objective often gives rise to a worsening in the performance of others. Even so, MOP has become a research hot spot due to its wide application in reality. A MOP (or MaOP) [19] is defined as:

$$\begin{aligned} &\min F(x) = (f_1(x), f_2(x), ..., f_m(x)) \\ &subject\ to\ x \in \Omega \end{aligned} \tag{1}$$

where $x = \{x_1, x_2, ..., x_n\}$ denotes a decision vector, Ω represents the decision space, and n indicates the dimensions of the decision vector. Because there are often conflicts between different objectives, there is no absolute or singular best solution, but rather a range of solutions that represent trade-offs between different objectives.

2.2. **Objective functions.**

In recent years, for image segmentation, many algorithms have considered only one or two objective functions. Aneesh introduced a new image segmentation approach called the differential evolutionary adaptive Harris Hawks optimization (DEAHHO) [20], which uses the Masi entropy function as the only objective

function. Bhandari suggested a color image thresholding segmentation approach based on a nature-inspired optimization methodology [21], with the Otsu and Kapur methods being employed in the optimization process. Sathya developed a new color image segmentation approach based on the Exchange Market algorithm [22], with the objective functions Kapur, Otsu, and Minimum Cross Entropy [23].

As shown above, it is infrequent to select more objective functions for image segmentation. By considering the quality of the image more comprehensively. In this study, we selected seven objective functions commonly used in the realm of image segmentation for multi-regional images to establish a seven-objective model. They are Otsu's function, Cross-Entropy function, Kapur's function, Tsallis entropic function [24], Fuzzy entropy function [25], Fuzzy C-means(FCM) function [26] and Rényi's entropy function [27].

2.3. **Particle swarm optimization.** The PSO belongs to a kind of swarm intelligence algorithm, which was proposed by Kennedy and Eberhart in 1995 and was designed by simulating the predatory behavior of a flock of birds [28]. Each particle in PSO represents a possible solution to the problem, it retains its position, velocity, and fitness values, which are calculated based on the fitness values in each iteration. Particle swarm algorithms have a wide range of applications and can be applied to many different fields. Based on this, researchers have applied PSO to image thresholding segmentation. Surina Borjigin used PSO to optimize t–Havrda–Charvát entropy and 2D histogram for color image segmentation [29]. Haixia proposed an image segmentation algorithm based on PSO and K-means algorithm for semantic segmentation of agricultural products [30]. In addition, to improve the hyper-parameters of GRP, a non-inertial particle swarm optimization with elite mutation-Gaussian process regression (NIPSO-GPR) method is presented [31].

In the frequently used PSO, each particle's position is renewed in each iteration in the light of its individual optimal position and the particle swarm's optimal solution. The following formula is used to refresh the particle's velocity and position:

$$v_i(t+1) = \omega \cdot v_i(t) + c_1 \cdot r_1 \cdot [pbest(t) - x_i(t)] + c_2 \cdot r_2 \cdot [gbest(t) - x_i(t)] \tag{2}$$

$$x_i(t+1) = x_i(t) + v_i(t+1) \tag{3}$$

where x is the particle's position, v is the particle's velocity, Ω represents inertia weight, *pbest* is the greatest position of the particle, *gbest* is the global greatest position of the swarm, r_1, r_2 are the random values in the range [0,1], c_1, c_2 are the cognitive coefficient.

2.4. **Information feedback model.** The updating procedure for persons in most MOP is a forward searching approach that does not employ previous personally identifiable information. Nonetheless, in the previous iteration, there was a large amount of good information. If that knowledge could be used successfully in the following optimization, the quality of the final solution could be significantly enhanced. The Information Feedback Model [32] is a simple fitness weighting method based on a basic algorithm that integrates information from prior iterations into the person in the current iteration for updating. This way, not only can the population's variety be preserved, but also the elite individuals can be retained, and the algorithm's computational efficiency can be increased. Many academics have merged the model with evolutionary algorithms because of its properties. There was abundant favorable information in the former iteration, if the favorable information can be used effectively in the subsequent. Yin introduced the information feedback model into MOEA/D [33]. The information feedback model has two methods of selecting individuals: fixed selection, and random selection. We used the information

feedback model that fixed a selection of individuals to the study for this paper. It is defined as follows:

$$x_i^t = \theta_1 \cdot x_i^{t-1} + \theta_2 \cdot y_i^t \tag{4}$$

$$\theta_1 = \frac{F_i^t}{F_i^t + f_i^{t-1}} \tag{5}$$

$$\theta_2 = \frac{f_i^{t-1}}{F_i^t + f_i^{t-1}} \tag{6}$$

where x_i^{t-1} represents the i th individual at the $(t-1)$ th generation, the fitness value of x_i^{t-1} is f_i^{t-1}. y_i^t represents the i th individual at the t th generation generated through the original algorithm and the fitness value of y_i^t *is* F_i^t. θ_1 and θ_2 are weight vectors inversely proportional to fitness values, and $\theta_1 > 0$, $\theta_2 > 0$ which satisfy $\theta_1 + \theta_2 = 1$.

3. **The proposed algorithm.** This section describes the specific steps of SMPSO-IFM. The core of SMPSO-IFM is to balance the conflicts between objective functions and improve the performance of the algorithm. The SMPSO is based on the original PSO algorithm with a speed limit and introduces a speed contraction mechanism. During the iteration of the particles, the position updates of particles in SMPSO are based on the position and velocity information of the previous generation of particles. In subsection 2.4, we described the information feedback model in detail. In order to make full use of the helpful information from the previous generation of particles, we fused the information feedback model with SMPSO to form the SMPSO-IFM algorithm. In the process of fusing the information feedback model, it is worthwhile to consider how to choose the fitness value of the particles. In this paper, we established a seven-objective model F(x) after considering the quality of images, and we selected the average fitness value for the calculation, and other users can adjust the weight of the fitness value according to their own needs. The flow chart of the proposed algorithm is as follows:

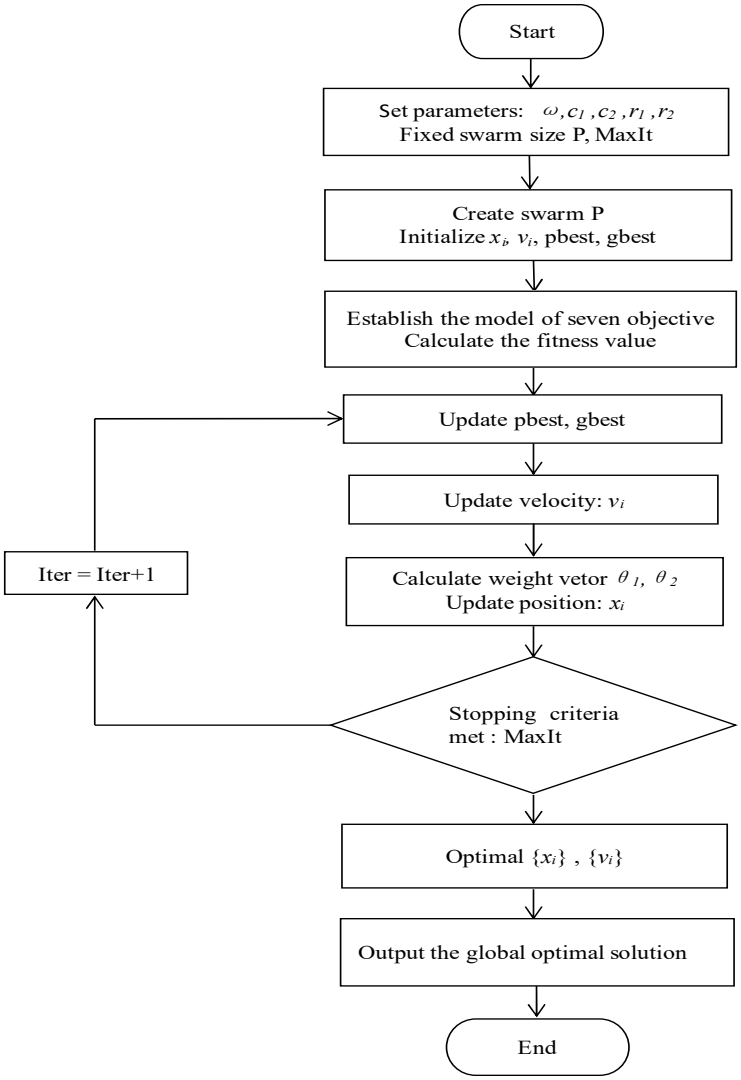

FIGURE 1. The flow diagram of the proposed method.

SMPSO-IFM's steps are listed below:
Step1: Set parameters ω, c_1, c_2, r_1, r_2, swarm size P, maximum iterations.
Step2: Initialize the position, velocity, the particles' pbest, the particles' gbest.
Step3: Establish the model of seven objective functions:

$$\begin{aligned} &\min F(x) = \begin{pmatrix} Fit_{Ots}(x), Fit_{Kap}(x), Fit_{MCE}(x), Fit_{Tas}(x), \\ Fit_{FE}(x), Fit_{FC}(x), Fit_{\mathrm{Re}n}(x) \end{pmatrix} \\ &subject\ to\ x \in \Omega \end{aligned} \tag{7}$$

The formula for each function is shown below:

$$Fit_{ots} = \sum_{i=0}^{L-1} W_i \cdot (\mu_i - \mu_w)^2 \tag{8}$$

$$Fit_{Kap} = \sum_{i=0}^{L-1} H_i \tag{9}$$

$$Fit_{MCE} = -\sum_{i=1}^{t-1} iP_i \log\left(\frac{i}{\mu\left(1,t\right)}\right) + \sum_{i=t}^{L} iP_i \log\left(\frac{i}{\mu\left(t,L+1\right)}\right) \tag{10}$$

$$Fit_{Tas} = S_q^A(t) + S_q^B(t) + \cdots + S_q^K(t) + \left((1-q)S_q^A(t)S_q^B(t)\cdots S_q^K(t)\right) \tag{11}$$

$$Fit_{_{FE}} = H_1 + H_2 + \cdots + H_n + H_{n+1} \tag{12}$$

$$Fit_{_{FC}}\left(U, t_1, t_2, \cdots t_k\right) = \sum_{i=1}^{K}\sum_{j=1}^{N_p} u_{ij}^{\tau} d_{ij}^2 \tag{13}$$

$$Fit_{_{Ren}} = \sum_{i=1}^{K} H_\alpha\left[C_i\right] \tag{14}$$

for specific parameter information, please refer to literature [7, 8, 20, 23, 24, 25, 27].

And then calculate the fitness value:

$$F_i^t = \frac{Fit_{Ots_i}^{\ t} + Fit_{Kap_i}^{\ t} + Fit_{MCE_i}^{\ t} + Fit_{Tas_i}^{\ t} + Fit_{FE_i}^{\ t} + Fit_{FCM_i}^{\ t} + Fit_{\mathrm{Re}n_i}^{\ t}}{7} \tag{15}$$

$$f_i^{t-1} = \frac{Fit_{Ots_i}^{\ t-1} + Fit_{Kap_i}^{\ t-1} + Fit_{MCE_i}^{\ t-1} + Fit_{Tas_i}^{\ t-1} + Fit_{FE_i}^{\ t-1} + Fit_{FCM_i}^{\ t-1} + Fit_{\mathrm{Re}n_i}^{\ t-1}}{7} \tag{16}$$

Step 4: Update pbest, gbest, and the velocity $vspacemathit{v}_i$.

Step 5: Update position x_i.

Step 5.1: Substitute Equation(15) and Equation(16) into Equation(5) and Eqation(6) to obtain the weight vector θ_1, θ_2.

Step 5.2: Update the position of the new generation of particles with the information feedback model, so we can rewrite Equation(3) as:

$$\overrightarrow{x}_i(t+1) = \theta_1 \cdot \overrightarrow{y}_i(t+1) + \theta_2 \cdot (\overrightarrow{x}_i(t-1) + \overrightarrow{v}_i(t)) \tag{17}$$

Step 6: Whether the conditions for termination have been met. If the termination conditions are not fulfilled, Iter = Iter+1, repeat step 3, and if the termination conditions are met, do step 7.

Step 7: Output. Output the segmentation result of the image.

The pseudocode of SMPSO-IFM is described in Algorithm 1.

4. **Experiments and results.** The first set of experiments carried out in this section examines the performance of SMPSO-IFM on images with various features, and the second uses benchmark problems to illustrate the superiority of SMPSO-IFM in the field of MaOP. The following is how the chapter is organized: The basic information about images is presented in Section 4.1, followed by performance metrics. Experimental parameter settings are given in Section 4.2. The results and comments are presented in Section 4.3. Benchmark priblems are given in Section 4.4. The algorithm's performance on the MAF and DTLZ test sets is presented in Sections 4.5 and 4.6.

Algorithm 1 Pseudocode of SMPSO-IFM

```
Input: Original images and the parameters
Output: The segmentation result of the image
initialize population size, dimension, maximum number of iterations, mutation probability crossover probability
initialize the position, velocity, pbest of the particles and gbest of the particles.
initializeLeadersArchive()
generation = 0
while generation < maxGenerations do
    computeSpeed()
    computeFitnessvalue() // Equation(15)-Equation(16)
    computeWeightvector() // Equation(5)-Equation(6)
    updatePosition() // Equation(17)
    mutation() // Turbulence
    evaluation()
    updateLeadersArchive()
    updateParticlesMemory()
    generation++
returnLeadersArchive()
```

4.1. **Quality of the segmented image.** The images in this paper are from BSDS(300) [34], this dataset is extensively used in many literatures as a reference tool for image segmentation and boundary detection. It includes 300 grayscale and natural color images. In this paper, we chose four images to show the segmentation results, each of which is 481×321 in size. These images have different characteristics.

In the face of various image processing methods, how to evaluate their segmentation quality becomes the most important problem. The Peak Signal to Noise Ratio (PSNR) [35] and the Structural Similarity (SSIM) [36] are two commonly utilized segmentation quality evaluation measures. The Feature Similarity (FSIM) [37] measure determines the degree of similarity between two images based on their internal features. The closer the SSIM value is to 1, the stronger image segmentation effect is. On the other hand, the PSNR criterion calculates the ratio of a signal's maximum possible power to the power of interfering noise. When the PSNR value is high, the segmentation quality improves. Although it is well known, it cannot replace human vision. The following is how PSNR is defined:

$$PSNR\,(x,y) = 20\log_{10}\left(\frac{255}{\sqrt{MSE\,(x,y)}}\right) \tag{18}$$

$$MSE(x,y) = \frac{1}{MN}\sum_{i=1}^{M}\sum_{i=1}^{N}(x(i,j)-y(i,j))^2 \tag{19}$$

We notice that $M \times N$ is the size of image I. The following is how SSIM is defined:

$$SSIM\,(x,y) = \frac{(2\mu_x\mu_y + C_1)\,(2\sigma_{xy} + C_2)}{\left(\mu_x^2 + \mu_y^2 + C_1\right)\left(\sigma_x^2 + \sigma_y^2 + C_2\right)} \tag{20}$$

where x and y represent the original and segmented images, μ_x and μ_y are the mean values, and σ_x and σ_y are the variances, σ_{xy} is the covariance. The constants C_1 and C_2 are used to maintain a stable the division with a weak denominator. Averaging the SSIM

values calculated across the entire neighborhoods of the original and segmented images produces the final SSIM value. The following is how FSIM is defined:

$$FSIM = \frac{\sum_{\omega\in\Omega} S_L(\omega)PC_m(\omega)}{\sum_{\omega\in\Omega} PC_m(\omega)} \tag{21}$$

$$S_L(\omega) = S_{PC}(\omega)PC_m(\omega) \tag{22}$$

$$S_pC(\omega) = \frac{2PC_1(\omega)PC_2(\omega) + T_1}{PC_1^2(\omega) + PC_2^2(\omega) + T_1} \tag{23}$$

$$S_G(\omega) = \frac{2G_1(\omega)G_2(\omega) + T_1}{G_1^2(\omega) + G_2^2(\omega) + T_1} \tag{24}$$

where ω is the gradient magnitude (GM) of an image, which is defined as:

$$G = \sqrt{G_x^2 + G_y^2} \tag{25}$$

$$PC(\omega) = \frac{E(\omega)}{(\varepsilon + \sum_n A_n(\omega))} \tag{26}$$

The magnitude of the response vector ω in on n is $E(\omega)$ and $A_n(\omega)$ is the scale's local amplitude, $n \cdot \varepsilon$ is a tiny positive number and $PC_m(\omega) = \max(PC_1(\omega), PC_2(\omega))$.

4.2. **Experimental settings.** In this section, the parameter settings of MaOP methods are given. These parameters can be divided into two categories. Firstly, they are common parameters for all MaOP algorithms, and the values of the parameters are kept constant during the experiments. The specific parameter settings are as follows: the population size N is set to 200, the maximum number of iterations is set to 1000, the dimension D is equivalent to the threshold, and in this paper we choosed the dimension 3 for the experiments. The other parameter settings of all algorithms in the experiments are shown in Table 1. c_1, c_2 are the specific parameters controlling the local optimal and full dramatic optimal subeffects, r_1, r_2 are random numbers belonging to between [0,1], and ω is the inertia weight of particles. xc is the simulated binary crossover distribution indicator (SBX), xm is the polynomial variance distribution indicator, pm represents the mutation probability, and pc represents the crossover probability. r_i is the random number belonging to [0,1] random factor and TF_i is the teaching factor belonging to [0,1].

Table 1. All algorithm specific parameters settings

Algorithm	Parameters settings
SMPSO-IFM	$1.5 < c_1$, $1.5 < c_2$, $r_1, r_2 \in [0,1]$, $\omega = 0.1$
KnEA	rate of knee points = 0.5, ratio of size of neighborhood = 1
NSGAIII-IFM	pc = 1, pm = 1/D, xc = 20,xm = 20
TLBO	$r_i \in [0,1]$, $TF_i \in [0,1]$
SMPSO/FCM	$1.5 < c_1$, $1.5 < c_2$, $r_1, r_2 \in [0,1]$, $\omega = 0.1$

In the model building process, we want to obtain a robust model. The robustness of a model can be understood as the model's tolerance to the degree of tolerance of data or parameter changes. A model is said to be robust if deviations in data or parameters have only a small effect on the output of the model, then the model is said to be robust. In order to verify the robustness of the model, the model parameters are varied in this paper. In the experimental process, the parameters c_1, c_2, r_1, r_2 are random numbers,

there is a great deal of uncertainty in the experimental processand. So the weight vector ω is changed to give the experimental results of four images, and the experimental errors are within 0.02. It is proved that the model has good robustness.

The experimental data plots are shown as follows:

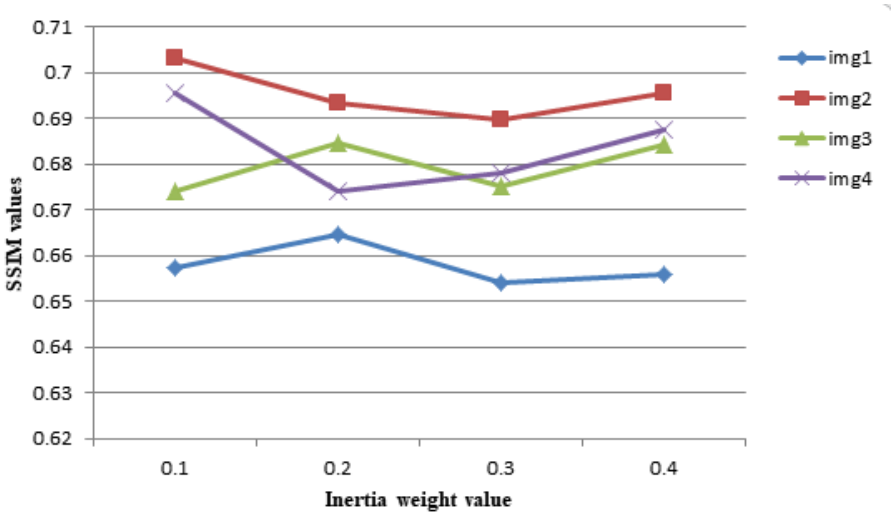

FIGURE 2. Experimental error comparison of four images under different parameters.

4.3. **Experiment result.** In this paper, SMPSO-IFM is used to optimize seven-objective model for image threshold segmentation, and the experimental results are compared with Knee Evolutionary Algorithm (KnEA) [38], NSGA III with information feedback model [39], Teaching-learning-based optimization (TLBO) [40] and SMPSO/FCM [41]. The segmentation quality of each method was evaluated by PSNR, SSIM, and FSIM. MATLAB was used to run the experiments on an Intel Core i5 with a 2.5 GHz processor. Figure 3 to Figure 6 show the results of the experiments.

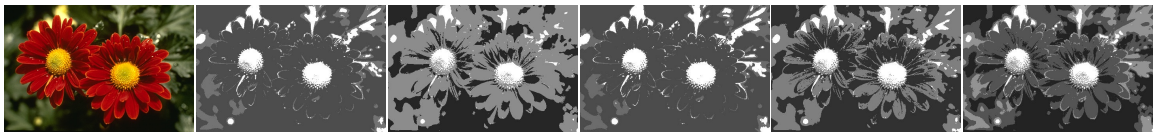

(a) (b) (c) (d) (e) (f)

FIGURE 3. Experimental results: (a) original image; (b) KnEA method; (c) NSGAIII method; (d) TLBO method; (e) SMPSO/FCM method; (f) SMPSO-IFM method.

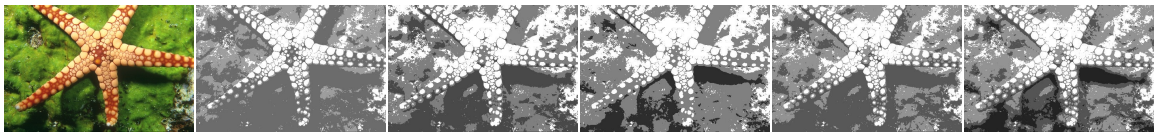

(a) (b) (c) (d) (e) (f)

FIGURE 4. Experimental results: (a) original image; (b) KnEA method; (c)NSGAIII method; (d) TLBO method; (e) SMPSO/FCM method ; (f) SMPSO-IFM method.

(a) (b) (c) (d) (e) (f)

FIGURE 5. Experimental results: (a) original image; (b) KnEA method; (c) NSGAIII method; (d) TLBO method; (e) SMPSO/FCM method segmentation; (f) SMPSO-IFM method.

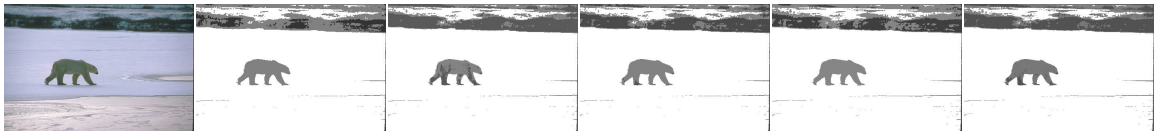

(a) (b) (c) (d) (e) (f)

FIGURE 6. Experimental results: (a) original image; (b) KnEA method; (c) NSGAIII method; (d) TLBO method; (e) SMPSO/FCM method; (f) SMPSO-IFM method.

The results of SMPSO-IFM compared with other MaOP methods on PSNR, SSIM, and FSIM metrics are shown in Table 2 to Table 6. The performance of five algorithms on an average of 100 images is shown in Table 2. The performance of the five algorithms for the standardized test images can be seen in Table 3 to Table 6. SMPSO-IFM is able to identify the greatest threshold for image segmentation. The tables show that the method proposed in this study outperformed all these other methods. On img4, we can see that SMPSO/FCM and the proposed method produce nearly identical results, but on other images, SMPSO-IFM outperforms other methods. When compared to the SSIM and FSIM, the proposed algorithm performs better on the test images. Overall, SMPSO-IFM outperforms the other four algorithms.

4.4. **Benchmark problems.** The SMPSO-IFM's performance is evaluated against the most most prevalently utilised benchmarks (MaF), where $D = 10$ is the decision variables number, and $M = 7$ is the objective functions number, $Iter = 10000$ is iterations number. After each group of experiments is run for 30 times independently, the average value is taken for comparison to verify the superiority of the SMPSO-IFM.

4.5. **Performance on MaF test suite.** This section looks at how all the algorithms perform on MaF1, MaF2, MaF5-MaF7, and MaF9-MaF12. The Inverted Generational Distance (IGD) [42] was chosen as the algorithm performance evaluation standard. The following is how IGD is defined:

$$IGD = \frac{\sum_{i-1}^{n} |d_i|}{n} \tag{27}$$

Table 2. Performance of five algorithms on the average of 100 images

	KnEA	NSGAIII-IFM	TLBO	SMPSO/ FCM	SMPSO-IFM
PSNR	13.2325	12.2843	13.0542	14.3761	16.0427
SSIM	0.5042	0.5122	0.5488	0.5885	0.6765
FSIM	0.6138	0.6045	0.6254	0.6751	0.7205

Table 3. Performance of five algorithms on image 1

	KnEA	NSGAIII-IFM	TLBO	SMPSO/ FCM	SMPSO-IFM
PSNR	14.6545	12.2557	14.2667	14.8273	17.6024
SSIM	0.5505	0.4365	0.5414	0.6079	0.7040
FSIM	0.7042	0.6144	0.6984	0.7241	0.7537

Table 4. Performance of five algorithms on image 2

	KnEA	NSGAIII-IFM	TLBO	SMPSO/FCM	SMPSO-IFM
PSNR	14.5234	14.0089	13.2517	14.6481	16.1698
SSIM	0.6408	0.5291	0.4881	0.5571	0.6641
FSIM	0.7143	0.6427	0.6071	0.6957	0.7318

Table 5. Performance of five algorithms on image 3

	KnEA	NSGAIII-IFM	TLBO	SMPSO/FCM	Proposed Method
PSNR	10.3022	11.6143	12.2224	14.0221	15.9010
SSIM	0.4179	0.5127	0.5578	0.5939	0.6013
FSIM	0.5023	0.5927	0.5974	0.5934	0.6098

Table 6. Performance of five algorithms on image 4

	KnEA	NSGAIII-IFM	TLBO	SMPSO/FCM	SMPSO-IFM
PSNR	12.4092	12.0524	12.3131	13.4193	13.5513
SSIM	0.6352	0.6105	0.6481	0.6165	0.6612
FSIM	0.6814	0.6468	0.6836	0.6575	0.7016

where n is the number of points in the Pareto Frontier and d_i represents the closest Euclidean distance between each point of the real frontier in the target space and the known frontier. The obtained results are presented in Table 7.

According to the experimental results, SMPSO-IFM outperforms KnEA, NSGAIII-IFM, TLBO on MaF2, MaF5, MaF6, and MaF11. But for MaF1 and MaF10, KnEA obtains better results than the SMPSO-IFM, which is not doing well. For MaF7 and MaF12, NSGAIII-IFM has achieved better results. TLBO has the best performance on MaF9. The results from the experiment show that SMPSO-IFM has significant advantages in MaOP. Figure 7 depicts the parallel coordinates of a non-dominant solution set of median IGD values derived by the comparison algorithm on a seven-objective MAF2 to illustrate the results.

TABLE 7. IGD values for KnEA, NSGAIII, TLBO and SMPSO-IFM on MaF. The best results on each line are shown in bold.

Problem	KnEA	NSGAIII-IFM	TLBO	SMPSO-IFM
MaF1	**2.0622e-01**	2.8447e-01	3.3527e-01	2.7543e-01
MaF2	2.1669e-01	2.2936e-01	2.0132e-01	**1.9950e-01**
MaF5	1.7522e+01	1.9937e+01	2.1789e+01	**1.4099e+01**
MaF6	2.0062e-02	2.0486e-02	5.9145e-02	**7.8427e-03**
MaF7	1.4094e+00	**7.0895e-01**	1.1786e+00	1.4637e+00
MaF9	4.6461e+00	5.6928e-01	**1.0784e+00**	4.5177e+00
MaF10	**1.1257e+00**	1.7786e+00	2.9887e+00	2.8744e+00
MaF11	1.0727e+00	1.1199e+00	1.2851e+00	**9.0483e-01**
MaF12	2.5122e+00	**2.5012e+00**	4.0798e+00	4.8011e+00

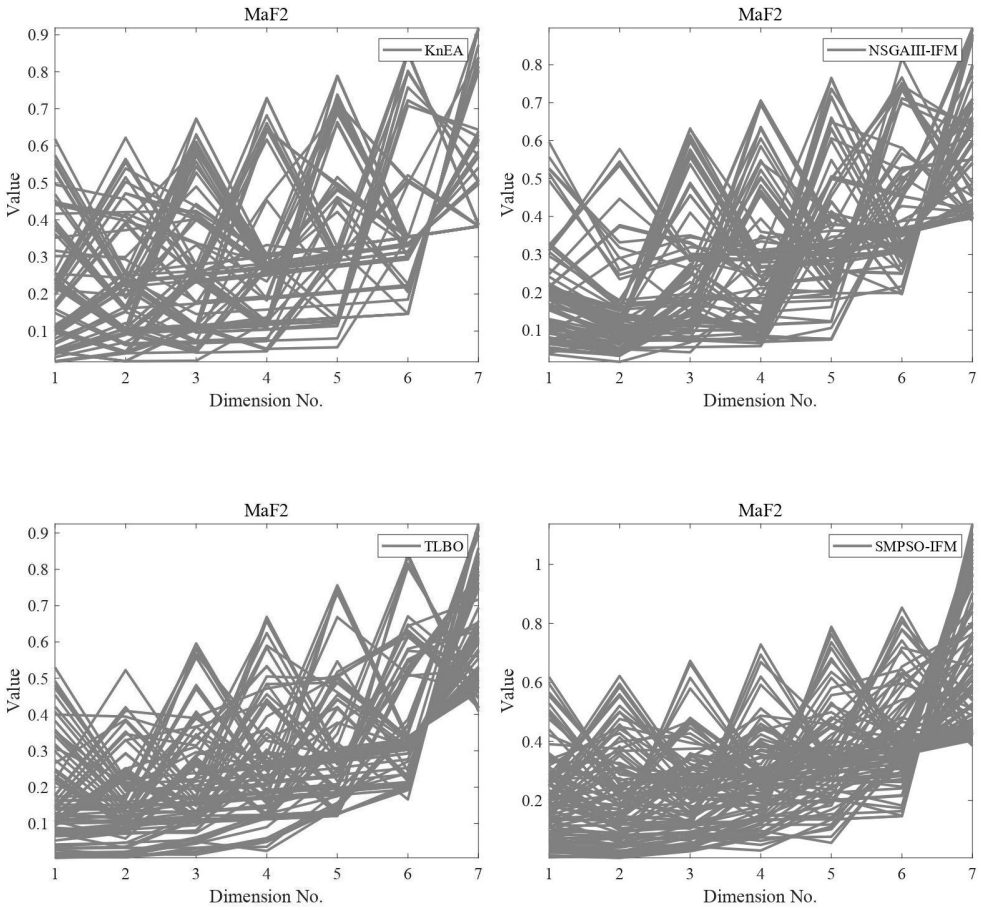

FIGURE 7. Nondominated front obtained by each algorithm on seven-objective MaF2 in the run associated with the IGD value.

4.6. **Performance on DTLZ test suite.** This section investigates the performance of all algorithms on DTLZ1-DTLZ6. We also chose the IGD as the evaluation criterion of algorithm performance. The obtained results are displayed in Table 8.

Experimentally, it is clear that SMPSO-IFM outperforms KnEA, NSGAIII-IFM, TLBO on DTLZ1, DTLZ4 and DTLZ5. But for DTLZ2, KnEA is the best. For DTLZ3 and DTLZ6, NSGAIII-IFM has achieved better results. The proposed algorithm's experimental results prove that it performs better when it comes to many-objective optimization.

TABLE 8. IGD values for KnEA, NSGAIII, TLBO and SMPSO-IFM on DTLZ. The best results on each line are shown in bold.

Problem	KnEA	NSGAIII-IFM	TLBO	SMPSO-IFM
DTLZ1	1.5849e+00	1.6312e+00	1.7665e+00	**7.4076e-01**
DTLZ2	**3.6669e-01**	5.1168e-01	7.1029e-01	6.6512e-01
DTLZ3	3.2563e+00	**9.2626e-01**	3.6416e+00	2.1649e+01
DTLZ4	4.7353e-01	5.5514e-01	5.8905e-01	**4.6322e-01**
DTLZ5	6.4721e-01	4.2437e-01	5.4682e-01	**4.1523e-01**
DTLZ6	9.7570e-01	**9.7042e-01**	2.0697e+00	1.1556e+01

To illustrate the results, Figure 8 plots the parallel coordinates of the non-dominated solution set with the median IGD value determined using DTLZ's seven-objective comparison algorithms.

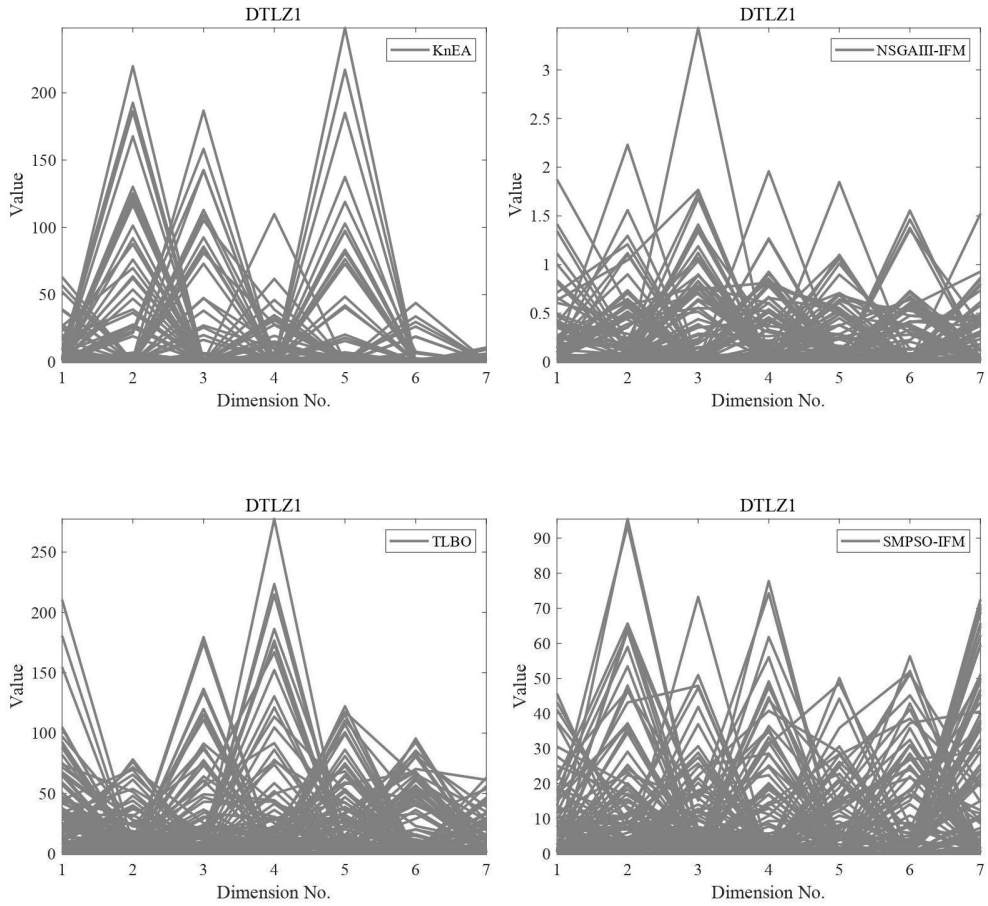

FIGURE 8. Nondominated front obtained by each algorithm on seven-objective MaF2 in the run associated with the IGD value.

5. **Conclusion.** In this research, a novel algorithm (SMPSO-IFM) is proposed for multi-regional image segmentation. Under the premise of considering the image quality, we established a seven-objective model belonging to MaOP. Because the performance of the algorithm degrades as the number of objective functions grows, the information feedback-based particle swarm algorithm is chosen to solve the model. The experiments demonstrate that the algorithm can produce high-quality segmented images. Furthermore, the

algorithm's performance is assessed utilizing benchmark problems from the MAF and DTLZ series. The performance is evaluated, and it is discovered that the proposed algorithm can improve the solution's convergence to the entire Pareto front, proving the algorithm's effectiveness.

This approach has the potential to be used in a variety of applications in the future, including: (1) Many-objective optimization is applied to different chemical fields. (2) Applied to handle many-objective engineering issues. (3) Improved classification regression by selecting the optimal set of features using many-objective methods. In the future, we can also consider combining image segmentation techniques with image encryption techniques [43, 44], and there are already many excellent image encryption research results to learn from.

Acknowledegment. This work is made possible by the National Key&D Program of China, Ministry of Science and Technology of the People's Republic of China (No 2020YFB1707804), and the Natural Science Foundation Project of science and Technology Department of Jilin Province under grant No. 20200201165JC.

REFERENCES

[1] M. A. E. Aziz, A. A. Ewees, A. E. Hassanien, "Whale Optimization Algorithm and Moth-Flame Optimization for multilevel thresholding image segmentation," *Expert Systems with Applications*, pp. 242–256, 2017.

[2] R. V. Menon, S. Kalipatnapu, I. Chakrabarti, "High speed VLSI architecture for improved region based active contour segmentation technique," *Integration the VLSI Journal*, vol. 77, pp. 25–37, 2021.

[3] C. Liu, W.-B. Liu, W.-W. Xing, "A weighted edge-based level set method based on multi-local statistical information for noisy image segmentation," *Journal of Visual Communication and Image Representation*, vol. 59, no. FEB., pp. 89–107, 2019.

[4] Q. Yu, C.-Z. Yang, H.-H. Fan, H.-J. Zhu, F.-Y. Ye, H. Wei, 'Bag of contour fragments for improvement of object segmentation," *Applied Intelligence*, vol. 50, no. 1, pp. 203–221, 2020.

[5] S.-H. Ren, Y.-X. Luo, T.-Y. Yan, L. Wang, D.-F. Chen, X.-L. Chen, "Machine learning-based automatic segmentation of region of interest in dynamic optical imaging," *AIP Advances*, vol. 11, no. 1, p. 010529, 2021.

[6] K. Hammouche, M. Diaf, P. Siarry, "A comparative study of various meta-heuristic techniques applied to the multilevel thresholding problem," *Engineering Applications of Artificial Intelligence*, vol. 23, no. 5, pp. 676–688, 2010.

[7] M. H. Merzban, E. Mahmoud, "Efficient Solution of Otsu Multilevel Image Thresholding: A Comparative Study," *Expert Systems with Applications*, vol. 116, 2019.

[8] T. Pun, "A new method for gray-level picture thresholding using the entropy of the histogram," *Signal Processing* , vol. 2, no. 3, pp. 223–237, 1985.

[9] J. Qin, X.-J. Shen, F. Mei, Z.Fang, "An Otsu multi-thresholds segmentation algorithm based on improved ACO," *The Journal of Supercomputing*, vol. 75, no. 2, pp. 995–967, 2019.

[10] B. Akay, "A study on particle swarm optimization and artificial bee colony algorithms for multilevel thresholding," *Applied Soft Computing*, vol. 13, no. 6, pp. 3066–3091, 2013.

[11] X.-Y. Xia, H. Gao, H.-D. Hu, R.-S. Lan, C.M. Pun, "A multi-level thresholding image segmentation based on an improved artificial bee colony algorithm," *Computers & Electrical Engineering*, vol. 70, pp. 931–938, 2018.

[12] D. Corne, J. Knowles, "Techniques for highly multiobjective optimisation: some nondominated points are better than others," *Proceedings of the 9th annual conference on Genetic and evolutionary computation*, pp. 773–780, 2007.

[13] M. Farina, P. Amato, "On the optimal solution definition for many-criteria optimization problems," *Fuzzy Information Processing Society, Nafips Meeting of the North American*, pp. 233–238, 2002.

[14] M. Karakoyun, S. Gulcu, H. Kodaz, "D-MOSG: Discrete multi-objective shuffled gray wolf optimizer for multi-level image thresholding," *Engineering Science and Technology an International Journal*, no. 3, 2021.

[15] K. Deb, A. Pratap, S. Agarwal, T. Meyarivan, "A fast and elitist multiobjective genetic algorithm: NSGA-II," *IEEE Transactions on Evolutionary Computation*, vol. 6, no. 2, pp. 182–197, 2002.
[16] K. Deb, H. Jain, "Evolutionary Many-Objective Optimization Algorithm Using Reference-Point Based Nondominated Sorting Approach, Part II: Handling Constraints and Extending to an Adaptive Approach," *IEEE Transactions on Evolutionary Computation*, vol.18, no. 4, pp. 602–622, 2014.
[17] M.-G. Gong, H. Li, D.-Y. Meng, Q.-G. Miao, J. Liu, "Decomposition-Based Evolutionary Multiobjective Optimization to Self-Paced Learning. Evolutionary Computation," *IEEE Transactions on Evolutionary Computation*, 2018.
[18] A.J. Nebro, "A new PSO-based metaheuristic for multi-objective optimization," *Proceedings of IEEE Symposium on Computational Intelligence in Miulti-Criteria Decision-Making*, 2009.
[19] A. Az, B. Yw, A. Jz, "Objective extraction via fuzzy clustering in evolutionary many-objective optimization," *Information Sciences*, vol. 509, pp. 343–355, 2020.
[20] A. Aw, A. Mkn, B. Rp, C. Bj, D. Aa, "A differential evolutionary adaptive Harris hawks optimization for two dimensional practical Masi entropy-based multilevel image thresholding," *Journal of King Saud University - Computer and Information Sciences*, 2020.
[21] A.K. Bhandari, A. Kumar, Singh, G. K, S. Chaudhary, "A novel color image multilevel thresholding based segmentation using nature inspired optimization algorithms," *Expert Systems with Application*, 2016.
[22] P. D. Sathya, R. Kalyani, V. P. Sakthivel, "Color Image Segmentation Using Kapur, Otsu and Minimum Cross Entropy Functions Based on Exchange Market Algorithm," *Expert Systems with Applications*, vol. 172, no. 3, pp. 114636, 2021.
[23] B. Lei, J.-L Fan, "Multilevel minimum cross entropy thresholding: A comparative study - ScienceDirect," *Applied Soft Computing*, 2020.
[24] M.A. El-Sayed, S. Abdel-Khalek, E. Abdel-Aziz, "Study of Efficient Technique Based On 2D Tsallis Entropy For Image Thresholding," *International Journal on Computer Science & Engineering*, vol. 3, no. 9, 2011.
[25] H.S. Naji, M. Al-Qaness, M.A. Elaziz, "Multi-level image thresholding based on modified spherical search optimizer and fuzzy entropy," *Entroy*, vol. 22, no. 3, p. 328, 2020.
[26] N.R. Pai, K. Pal, J.M. Keller, J.C. Bezdek, "A possibilistic fuzzy c-means clustering algorithm," *IEEE Transactions on Fuzzy Systems*, vol. 13, no. 4, pp. 517–530, 2005.
[27] W. Liu, Y. Huang, Z. Ye, W. Gai, S. Yang, X. Cheng,, "Renyi's Entropy Based Multilevel Tresholding Using a Novel Meta-Heuristics Algorithmm," *Applied Sciences* , vol. 10, no. 9, pp. 3225, 2020.
[28] J. Kennedy, R. Eberhart, "Particle Swarm Optimization," *Icnn95-international Conference on Neural Networks*, IEEE, 1995.
[29] S. Borjigin, P.K. Sahoo, "Color image segmentation based on multi-level Tsallis–Havrda–Charvát entropy and 2D histogram using PSO algorithms," *Pattern Recognition*, vol. 92, pp. 107–118, 2019.
[30] A. Hz, B. Qp, "PSO and K-means-based semantic segmentation toward agricultural products," *Future Generation Computer Systems*, 2021.
[31] L.-L. Kang, R.-S. Chen, N. Xiong, Y.-C. Chen, Y.-X. Hu, C.-M. Chen, "Selecting Hyper-Parameters of Gaussian Process Regression Based on Non-Inertial Particle Swarm Optimization in Internet of Things," *IEEE Access*, vol. 7, pp. 59504–59513, 2019.
[32] G.-G. Wang, Y. Tan, "Improving Metaheuristic Algorithms With Information Feedback Models," *IEEE Transactions on Cybernetics*, vol. PP, no. 99, pp. 1–14, 2017.
[33] Y. Zhang, G.-G. Wang, K.-Q. Li, C. Wcy, D. Mj, A. Jd, " Enhancing MOEA/D with information feedback models for large-scale many-objective optimization - ScienceDirect," *Information Sciences*, vol. 522, pp. 1–16, 2020.
[34] D. Martin, C. Fowlkes, D. Tal, J. Malik, "A database of human segmented natural images and its application to evaluating segmentation algorithms and measuring ecological statistics," *IEEE International Conference on Computer Vision*, IEEE, 2002.
[35] Q. Huynh-Thu, M. Ghanbari, "Scope of validity of PSNR in image/video quality assessment," *Electronics Letters*, vol. 44, no. 13, pp. 800–801, 2008.
[36] Z. Wang, A.C. Bovik, H.R. Sheikh, E.P. Simoncelli, "Image quality assessment: from error visibility to structural similarity," *IEEE Transactions on Image Processing*, vol. 13, no. 4, 2004.
[37] U. Sara, M. Akter, M.S. Uddin, "Image Quality Assessment through FSIM, SSIM, MSE and PSNR—A Comparative Study," *Journal of Computer and Communications*, vol. 7, no. 3, pp. 11, 2019.
[38] M. A. Elaziz, S. Lu, "Many-objectives Multilevel Thresholding Image Segmentation using Knee Evolutionary Algorithm," *Expert Systems with Applications*, vol. 125, pp. 305–316, 2019.

[39] Z.-M. Gu, G.-G. Wang, "Improving NSGA-III algorithms with information feedback models for large-scale many-objective optimization," *Future Generation Computer Systems*, vol. 107, pp. 49–69, 2020.

[40] H.S. Gill, B.S. Khehra, A. Singh, L. Kaur, "Teaching-learning-based optimization algorithm to minimize cross entropy for Selecting multilevel threshold values," *Egyptian Informatics Journal*, vol. 20, no. 1, pp. 11–25, 2019.

[41] Z. Lu, Y. Qiu, Y. Fu, B. Lu, "An improved FCM method for image segmentation based on wavelet transform and particle swarm," pp. 112–117, 2018.

[42] C.A. Rodríguez Villalobos, C.A.Coello Coello, "A new multi-objective evolutionary algorithm based on a performance assessment indicator," *Conference on Genetic & Evolutionary Computation*, p.505, 2012.

[43] M. Samiullah, W. Aslam, M.A. Khan, H.M. Alshahrani, H. Mahgoub, A. M. Abdullah, M. Ullah, C.-M. Chen, "Rating of Modern Color Image Cryptography: A Next-Generation Computing Perspective," *Wireless Communications and Mobile Computing*, 2022.

[44] T.-Y. Wu, X.-N. Fan, K.-H. Wang, J.-S. Pan, C.-M. Chen, "ecurity Analysis and Improvement on an Image Encryption Algorithm Using Chebyshev Generator," *Journal of Internet Technology*, vol. 20, no. 1, pp. 13–23, 2019.

[45] H.-C. Huang, J.-S. Pan, Y.-H. Huang, F.-H. Wang, and K.-C. Huang, "Progressive watermarking techniques using genetic algorithms," *Circuits, Systems, and Signal Processing*, vol. 26, no. 5, pp. 671–687, 2007.

[46] T.-Y. Wu, Z. Lee, L. Yang, and C.-M. Chen, "A provably secure authentication and key exchange protocol in vehicular ad hoc networks," *Security and Communication Networks*, vol. 2021, 9944460, 2021.

[47] T.-Y. Wu, Q. Meng, L. Yang, X. Guo, and S. Kumari, "A provably secure lightweight authentication protocol in mobile edge computing environments," *The Journal of Supercomputing*, 2022. [Online]. Available: https://doi.org/10.1007/s11227-022-04411-9

[48] H.-C. Huang, J.-S. Pan, and C.-M. Chu, "Optimized copyright protection systems with genetic-based robust watermarking," in *Third International Conference on Intelligent Information Hiding and Multimedia Signal Processing (IIH-MSP 2007)*. IEEE, 2007, pp. 465–468.

[49] J.-S. Pan, H.-C. Huang, L. C. Jain, and W.-C. Fang, *Intelligent Multimedia Data Hiding: New Directions*, Springer Berlin, Heidelberg, 2007.

[50] A. Buriro, "Behavioral biometrics for smartphone user authentication," Ph.D. dissertation, University of Trento, 2017.